Acta Crystallographica Section B
Structural Science
ISSN 0108-7681

Investigation of diffraction line broadening due to compositional fluctuations in L-alanine-doped triglycine sulfate

Rajul Ranjan Choudhury,* R. Chitra and M. Ramanadham

Solid State Physics Division, Bhabha Atomic Research Center, Trombay, Mumbai 400085, India

Correspondence e-mail: rajul-ranjan@indiatimes.com

Received 18 February 2003
Accepted 10 July 2003

Broadening of X-ray powder diffraction peaks as a result of compositional disorder in L-alanine-doped triglycine sulfate crystals is investigated using the Williamson–Hall method. The analysis indicates that L-alanine substitution in triglycine sulfate crystals leads to anisotropic strain in the crystal.

1. Introduction

Triglycine sulfate (TGS), $[NH_3^+CH_2COO^-][NH_3^+CH_2COOH]_2\cdot SO_4^{2-}$, is a room-temperature ferroelectric that is used extensively in the field of radiation detection because of its pyroelectic nature. The ferroelectric phase-transition temperature (T_c) of TGS is 322 K, and the space groups below and above T_c are $P2_1$ and $P2_1/m$, respectively (Jona & Shirane, 1962). The asymmetric unit of the TGS unit cell contains three glycine molecules, denoted GI, GII and GIII, and a sulfate ion (Fig. 1).

In the ferroelectric phase (*i.e.* for $T < T_c$), an unpoled TGS crystal is divided into domains. There are two types of domains in TGS, which have opposite spontaneous polarization directions, and these directions can be reversed by application of an electric field. For radiation detection a single-domain single crystal of TGS is required, which is obtained either by applying an external electric field to a TGS crystal or by using a crystal that has an internal bias field. Previous studies (Bye *et al.*, 1972) have shown that one of the most effective ways of creating an internal bias in TGS crystals is to dope them with alanine (NH_2CHCH_3COOH), which is an amino acid similar to glycine (NH_2CH_2COOH), the only difference between the two being the presence of a $-CH_3$ group in alanine in place of one of the two α H atoms of glycine. Alanine exists in two enantiomorphic forms, *viz.* L-alanine and D-alanine. Because of the similarity between alanine and glycine, it was believed that alanine partially replaces one of the three glycine molecules (GI, GII or GIII) in TGS (Bye *et al.*, 1972; Keve *et al.*, 1971), and hence the doped crystals should contain two types of molecules, namely triglycine sulfate molecules, $(glycine)_3\cdot SO_4$, and modified molecules, $(glycine)_2\cdot(alanine)\cdot SO_4$. The word 'molecule' is taken to include the entire formula unit. In one of the two types of domains in TGS, L-alanine replaces a glycine group, *i.e.* the modified molecule is $(glycine)_2\cdot(L\text{-}alanine)\cdot SO_4$, and in the other domain D-alanine replaces a glycine group, *i.e.* the modified molecule is $(glycine)_2\cdot(D\text{-}alanine)\cdot SO_4$. This hypothesis was confirmed experimentally (Keve *et al.*, 1971) by the observation that L-alanine and D-alanine doping in TGS result in internal bias fields of opposite directions. Steric considerations, in accordance with the principle of selective additive adsorption and

eventual possible occlusion described by Weissbuch *et al.* (1991), decide the most likely sites of substitution of the modified molecule in the crystal.

The presence of a $(glycine)_2{\cdot}(alanine){\cdot}SO_4$ molecule in a unit cell freezes the spontaneous polarization direction of that particular unit cell, *i.e.* it is not possible to reverse the polarization direction of such a unit cell by applying an electric field. Such unit cells act as irreversible dipoles that polarize the surrounding unit cells, and as the number of such unit cells increases, the population of domains having a favourable spontaneous polarization direction increases at the expense of the other domain, thereby making the crystal more or less single domain (Keve *et al.*, 1971). Since an alanine molecule is larger than a glycine molecule, substitution of an alanine molecule for a glycine molecule will lead to local stresses and lattice distortions in the TGS crystals. The present diffraction study aims to investigate the effects of L-alanine substitution on TGS diffraction peaks.

2. Theoretical background

The observed profile, $h(x)$, of an X-ray powder diffraction (XRPD) peak is a convolution of two contributions, *viz.* the instrument contribution, $g(x)$, and the sample contribution, $s(x)$

$$h(x) = g(x)\, s(x). \qquad (1)$$

The wavelength distribution and geometric aberrations are usually treated as characteristic of a particular instrument, the instrument profile, $g(x)$, giving the peak profile for an ideal sample with no specimen broadening. There are two main origins of specimen broadening; firstly, there is broadening owing to the finite crystallite size (also called size broadening), and secondly, dislocations, vacancies, interstitials, substitutions and similar defects in the crystallites result in lattice strains that lead to strain broadening of the diffraction peaks.

The Warren–Averbach (Warren & Averbach, 1950, 1952) and integral-breadth (Williamson & Hall, 1953) procedures are the most commonly used methods of line-profile analysis. Of these two methods, the Warren–Averbach method is a more detailed approach to complete line-profile analysis. However, this method has a very serious drawback in cases where substantial line overlap and weak structural broadening occur; in such cases, the integral-breadth method is better.

TGS is an organic compound with 37 atoms in the asymmetric unit, a large unit cell (a = 9.417, b = 12.643, c = 5.735 Å and β = 110.4°) and low symmetry (monoclinic), and hence there is significant overlap of the powder peaks of TGS at the Cu $K\alpha$ wavelength (Fig. 2). Therefore, the integral-breadth

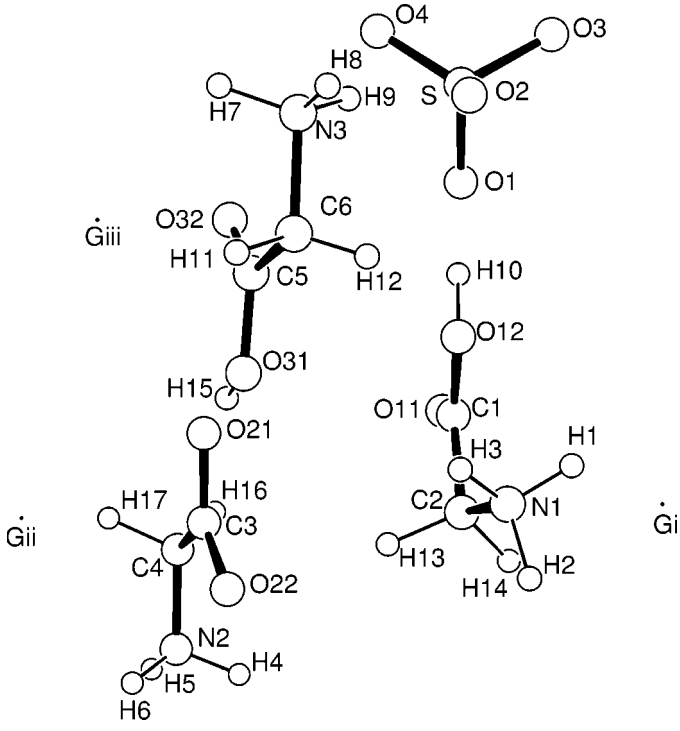

Figure 1
The asymmetric unit of the TGS unit cell.

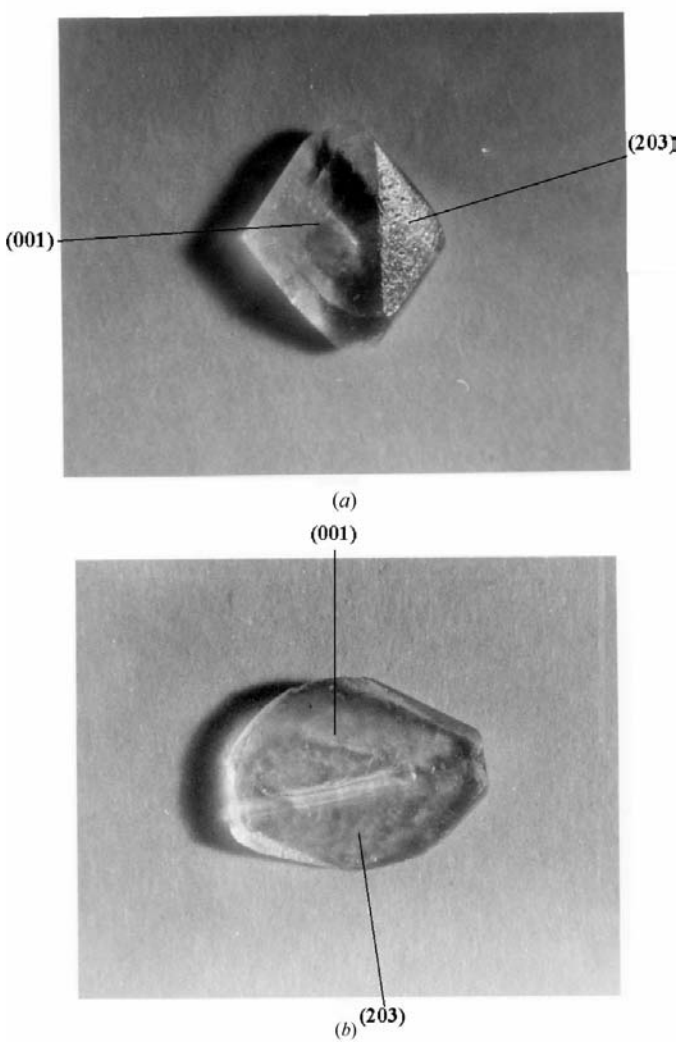

Figure 2
Photographs of (*a*) a LATGS(x = 0) crystal and (*b*) a LATGS(x = 0.25) crystal.

method was used for the line-profile analysis of the XRPD patterns of TGS presented here.

According to the Williamson–Hall method, the sample contribution to the integral-breadth (β) of the diffraction peak can be written as

$$\beta(\text{sample}) = \beta(\text{size}) + \beta(\text{strain}) \quad (2)$$

[this expression holds for a Lorentzian specimen profile, $s(x)$], where β(size) and β(strain) are the size and strain contributions, respectively. β(size) is given by the Scherrer formula (Stokes & Wilson, 1942, 1944)

$$\beta(\text{size}) = K\lambda/D\cos\theta, \quad (3)$$

where D is the average value of the volume of crystallite present in the powder and K is the Scherrer constant ($1.0 > K > 0.89$). Strain (ε) broadening is given by the equation

$$\beta(\text{strain}) = 0.4\,\varepsilon\tan\theta, \quad (4)$$

and hence

$$\beta(\text{sample}) = K\lambda/D\cos\theta + 4\,\varepsilon\tan\theta. \quad (5)$$

The intercept of the linear fit between β(sample)cosθ and sinθ gives an estimate of D, and the slope gives an estimate of the average strain (ε).

The powder diffraction pattern-analysis software *SHADOWV2*, developed by S. A. Howard (Department of Ceramic Engineering, University of Missouri, USA), was used in this study. First, the instrument calibration curve was obtained by analysing the powder pattern of a standard sample recorded at the instrument. The program performs a numerical convolution of the instrument profile WG (generated using the instrument calibration curve) with the sample profiles which can be Lorentzian, Gaussian or a combination of both. A point in the convoluted profile is obtained using the following numerical integration

$$W\,G\,S(i) = \sum_{j=-l}^{j=l} [W\,G(i+j)\,S(j)]. \quad (6)$$

Since the specimen profile is symmetric, j runs from $-l$ to l, where l is the number of points from the peak to the limits of the tails. The parameters refined by the program include the Bragg angle 2θ for the Cu $K\alpha_1$ wavelength, the integral-breadth of the specimen profile and the intensity of the convoluted profile.

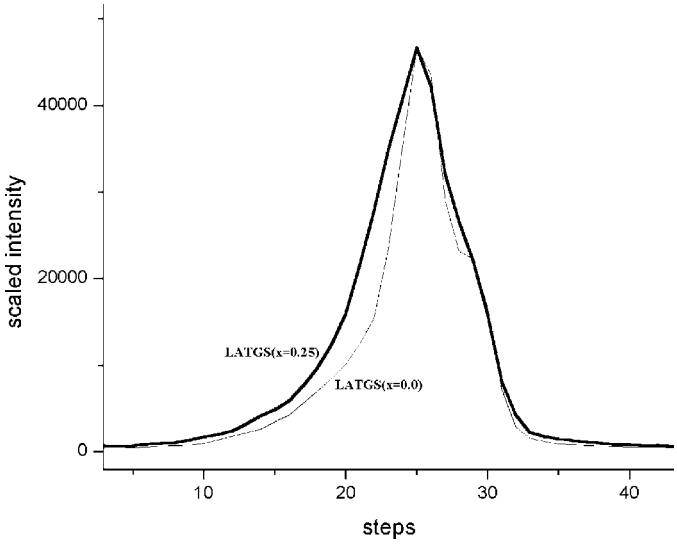

Figure 4
The (040) peaks of LATGS(x = 0) and LATGS(x = 0.25); the intensity of the LATGS(x = 0.25) peak has been scaled to show the increase in the width of the diffraction peak.

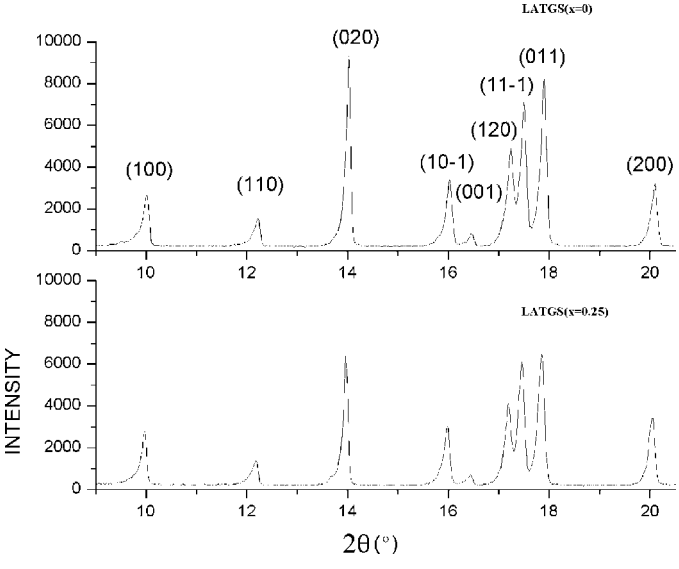

Figure 3
XRPD patterns of LATGS(x = 0) (top) and LATGS(x = 0.25) (bottom).

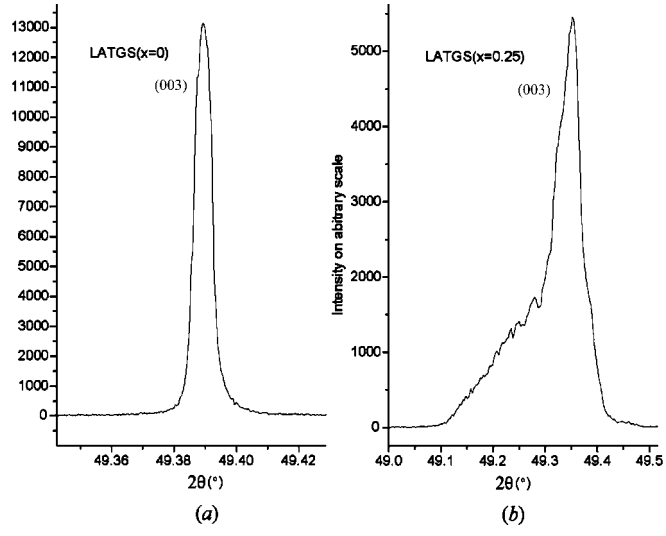

Figure 5
(*a*) The (003) Bragg peak for the LATGS(x = 0) single crystal. (*b*) The (003) Bragg peak for the LATGS(x = 0.25) single crystal.

Table 1
Results of the Williamson–Hall analysis when the instrument profile *WG* was generated using the calibration curve obtained after peak-shape analysis of the XRPD pattern of a standard Si sample.

Sample	Average crystallite size (nm)	Average crystallite strain	Residual error (%)
LATGS($x = 0$)	127 (32)	0.00005 (55)	19.82
LATGS($x = 0.25$)	159 (44)	0.00066 (2)	16.84

Table 2
Results of the Williamson–Hall analysis when the instrument profile *WG* was generated using the calibration curve obtained after peak-shape analysis of the XRPD patterns of a pure TGS sample.

Sample	Average crystallite size (nm)	Average crystallite strain	Residual error (%)
LATGS($x = 0$)	4000	0.0000 (6)	8.97
LATGS($x = 0.25$)	4000	0.0005 (4)	8.77

3. Experimental procedure

A series of crystals of L-alanine-doped triglycine sulfate (LATGS) were grown from aqueous solutions prepared from glycine, L-alanine and sulfuric acid according to the formula $(\text{glycine})_{3(1-x)}\cdot(\text{L-alanine})_{3x}\cdot H_2SO_4$, by allowing the solution to evaporate slowly at a constant temperature of 300 K. The crystals were harvested after precipitation of a small fraction of the dissolved solvate. Crystals with $x = 0$, 0.1, 0.15 and 0.25 were grown; the actual percentage of L-alanine entering the crystal is always less than that (x) in the solution. Fig. 2 shows photographs of the LATGS($x = 0$) and LATGS($x = 0.25$) crystals.

XRPD patterns (Fig. 3) of these LATGS crystals were scanned using a Rigaku diffractometer with a Cu $K\alpha$ source. The time per step for the recorded patterns was 6 s and the step size was 0.02°.

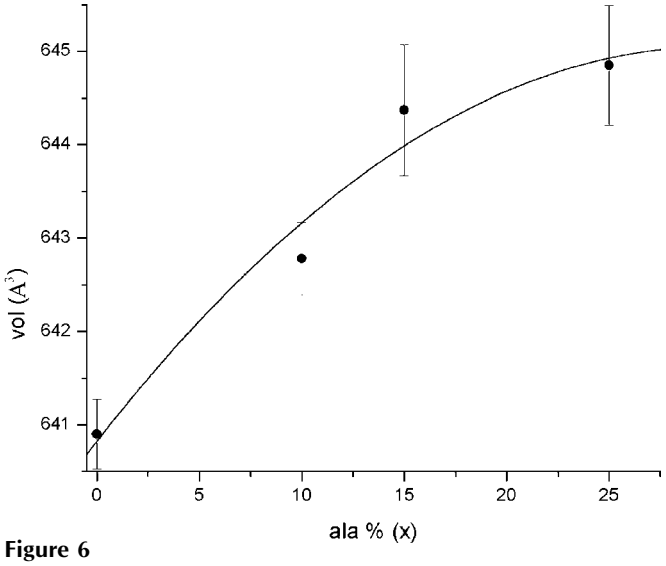

Figure 6
The variation of the average unit-cell volume of LATGS crystals with alanine concentration (x) in solution.

Fig. 4 gives a comparison between the (040) peaks of LATGS($x = 0$) at $2\theta = 28.22°$ and LATGS($x = 0.25$) at $2\theta = 28.18°$. A significant increase in the peak width of LATGS($x = 0.25$) compared with that of LATGS($x = 0$) was observed.

A high-resolution X-ray diffraction pattern of a standard silicon sample provided by Rigaku was recorded on a Rigaku X-ray powder diffractometer in order to obtain the instrument calibration curve.

A high-resolution Philips X'Pert-MRD diffractometer was used to record a Bragg reflection from the LATGS($x = 0$) and LATGS($x = 0.25$) single crystals. One of the prominent natural faces [with index (00l)] of the two single crystals shown in Fig. 2 was brought to the diffracting position and the Bragg peak

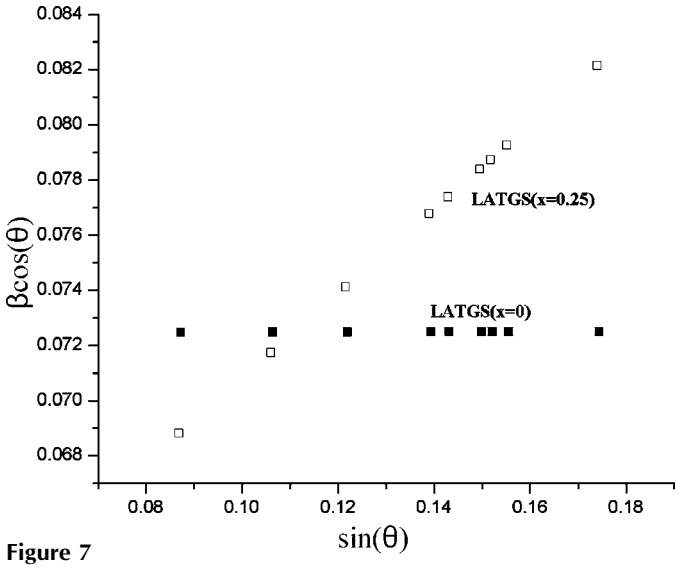

Figure 7
$\beta\cos\theta$ *versus* $\sin\theta$ for the LATGS($x = 0$) and LATGS($x = 0.25$) samples, where the XRPD pattern of a standard Si sample was used to generate the instrument calibration curve.

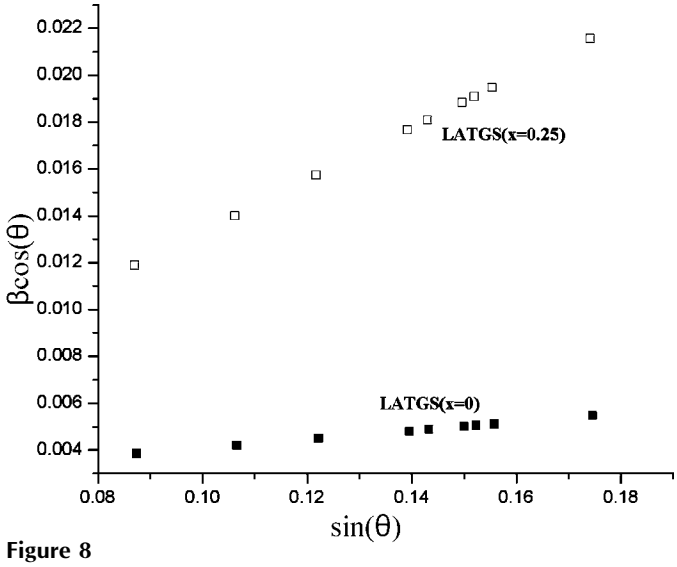

Figure 8
$\beta\cos\theta$ *versus* $\sin\theta$ for the LATGS($x = 0$) and LATGS($x = 0.25$) samples, where the XRPD pattern of a pure TGS sample was used to generate the instrument calibration curve.

Table 3
Average strain (ε) for a given *hkl* index.

hkl	LATGS(x = 0.25) strain (ε)	Residual error (%)
(100)	0.0000	8.58
(110)	0.0007 (2)	6.91
(020)	0.0000	12.31
(10$\bar{1}$)	0.0007 (1)	7.26
(001)	0.0007 (1)	7.26
(120)	0.00040 (6)	4.75
(11$\bar{1}$)	0.00040 (6)	4.75
(011)	0.00040 (6)	4.75
(200)	0.0000	8.42

was recorded. Fig. 5 shows the (003) peak from the LATGS(x = 0) and LATGS(x = 0.25) crystals. It is clear from the comparison of these two peaks that, in the case of LATGS(x = 0.25), there is more than one d spacing for the (003) plane, because there are regions in the crystal where the unit cells have expanded as a result of the presence of the modified molecule (glycine)$_2$·(L-alanine)·SO_4.

4. Results of the Willamson–Hall analysis

The instrument calibration curve was generated using the program *INSCALV*2, which is part of the *SHADOWV*2 package. A split Pearson VII function was used to model the instrument peak profile; the shape parameter and the FWHM for the $K\alpha_2$ and $K\alpha_3$ wavelengths were assumed to be the same as those for the $K\alpha_1$ wavelength.

Indexing of the LATGS XRPD patterns and cell-parameter refinement were performed using *PINDEX* (Boultif & Louer, 1991). Fig. 6 shows the variation of the average unit-cell volume with L-alanine percentage (x) in LATGS crystals. The average unit-cell volume increases proportionally with x for small values of x but saturates beyond $x \simeq 0.15$. This behaviour indicates that, initially, more and more alanine enters the crystal as the alanine percentage in solution (x) is increased, but beyond the limit, the increase in alanine percentage in solution does not result in a proportional increase in the intake of alanine into the crystals.

The first nine peaks of the LATGS patterns shown in Fig. 3, with *hkl* indices of (100), (110), (020), (10$\bar{1}$), (001), (120), (11$\bar{1}$), (011) and (200), were used for this analysis, as the peak overlap in this 2θ region was not very critical. The specimen profile (S) was taken to be Lorentzian. The values of average strain and average crystallite size obtained from the Williamson–Hall analysis for LATGS samples with x = 0 and x = 0.25 are given in Table 1, and Fig. 7 shows a plot of $\beta\cos\theta$ *versus* $\sin\theta$ for the LATGS(x = 0) and LATGS(x = 0.25) samples. The D values for the two samples are comparable, but the average strain in LATGS(x = 0.25) is more than ten times that in LATGS(x = 0). The increase in internal strain in the LATGS(x = 0.25) crystals is attributed to alanine substitution. Unit cells in which one of the TGS molecules is replaced by a (glycine)$_2$·(L-alanine)·SO_4 modified molecule expand in order to accommodate the larger molecule and, as a result, local stress is introduced into the region around these

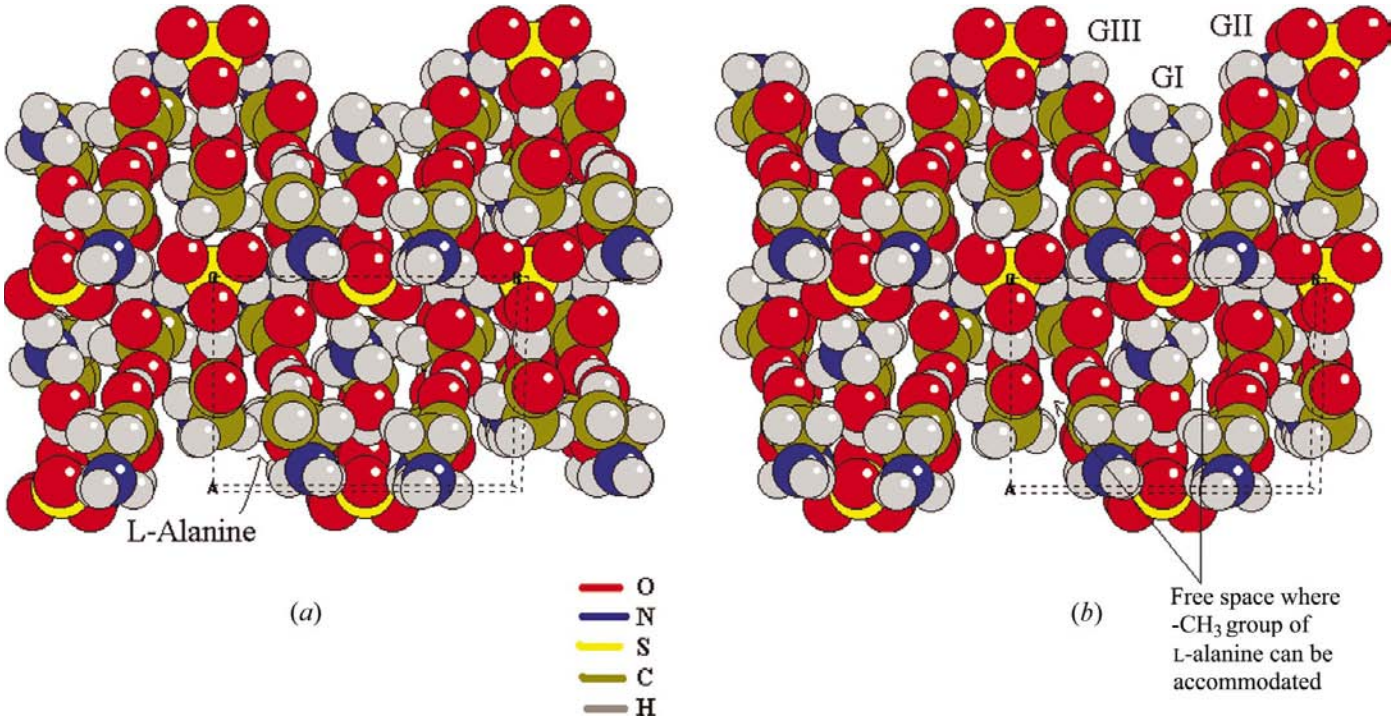

Figure 9
(*a*) Unit-cell packing in a LATGS crystal in which glycine at GII is completely replaced by L-alanine. (*b*) The unit-cell packing in a TGS crystal.

unit cells. The presence of a number of such unit cells in the crystals results in a net internal strain within the crystal.

With the intention of comparing the peak profiles of the doped TGS samples with those of a pure TGS sample, a calibration curve was generated assuming pure TGS to be the standard. The Williamson–Hall analysis was repeated, with *WG* in this case representing the pure TGS profiles and *S* giving the specimen broadening, the source of which was the presence of defects in the doped samples. *S* was taken to be Lorentzian. The results of this analysis are given in Table 2, and Fig. 8 shows a plot of $\beta\cos\theta$ *versus* $\sin\theta$ for the LATGS($x = 0$) and LATGS($x = 0.25$) samples. It is clear from these results that crystallite strain resulting from compositional fluctuation is the principal cause of peak broadening in LATGS crystals. The average strain for all nine of the *hkl* planes was calculated using (4), and the results are given in Table 3. It is evident from these results that the strain is anisotropic and *hkl* dependent. This result is in accordance with the marked anisotropic behaviour of the linear compressibility of TGS (Dunk & Saunders 1984); TGS crystals are known to be more easily strained along the [001] direction than the [010] and [100] directions.

5. Discussion

Our previous single-crystal neutron diffraction study (Choudhury *et al.*, 2002) conducted on LATGS crystals indicated that L-alanine partially replaces zwitterionic glycine at the GII site in TGS (Fig. 1). Figs. 9(*a*) and (*b*) show the packing in a hypothetical LATGS crystal in which glycine at GII has been completely replaced by L-alanine and a TGS crystal, respectively. It is clear from a comparison of Figs. 9(*a*) and (*b*) that the substitution of alanine for glycine leads to an increase in the packing density of the unit cell, since the free space between GI and GII in TGS becomes occupied by the $-CH_3$ group of L-alanine in the LATGS crystal. The values of the packing coefficient (molecular volume/unit-cell volume) for the pure TGS unit cell and the unit cell of a doped crystal in which one of the two TGS molecules is replaced by the modified molecule $(\text{glycine})_2\cdot(\text{L-alanine})\cdot SO_4$, calculated assuming the unit-cell volume to be 640 Å^3 (volume of pure TGS unit cell), are 0.86 and 0.90, respectively [*MOLDRAW* (Ugliengo *et al.*, 1993) was used to calculate the molecular volumes]. In order to decrease the packing density of the substituted unit cell, the cell has to expand, which results in straining of the adjacent unit cells. The presence of such larger-volume unit cells in the crystal leads to net internal strain in the entire crystal; the number of such unit cells present in the crystal depends on the doping level. Hence, alanine substitution in TGS leads to internal strains in the crystal and this strain results in the broadening of the diffraction lines recorded using a high-resolution diffractometer.

The authors would like to thank Professor K. S. Chandrashekhar for making the high-resolution X-ray diffractometer X'Pert-MRD, located at Tata Institute for Fundamental Research, available for this work and for his valuable guidance and suggestions. They would also like to thank Mr B. Wanjari of RB&HSD, Bhabha Atomic Research Centre, for providing photographs of the crystals.

References

Boultif, A. & Louer, M. (1991). *J. Appl. Cryst.* **24**, 987–993.
Bye, K. L., Whipps, P. W. & Keve, E. T. (1972). *Ferroelectrics*, **4**, 253–256.
Choudhury, R. R., Chitra, R., Ramanadham, M. & Javeyl, R. (2002). *Appl. Phys. A*, **74**, S1667–S1669.
Dunk, A. & Saunders, G. A. (1984). *J. Mater. Sci.* **19**, 125–134.
Jona, F. & Shirane, G. (1962). In *Ferroelectric Crystals.* Oxford/London: Pergaman Press.
Keve, E. T., Bye, K. L., Whipps, P. W. & Annis, A. D. (1971). *Ferroelectrics*, **3**, 39–48.
Stokes, A. R. & Wilson, A. J. C. (1942). *Proc. Cambridge Philos. Soc.* **38**, 313.
Stokes, A. R. & Wilson, A. J. C. (1944). *Proc. Cambridge Philos. Soc.* **40**, 197.
Ugliengo, P., Barzani, G. & Viterbo, D. (1993). *Z. Kristallogr.* **207**, 9.
Warren, B. E. & Averbach, B. L. (1950). *J. Appl. Phys.* **21**, 595–599.
Warren, B. E. & Averbach, B. L. (1952). *J. Appl. Phys.* **23**, 497.
Weissbuch, I., Addadi, L., Lahav, M. & Leiserowitz, L. (1991). *Science*, **253**, 637–639.
Williamson, G. K. & Hall, W. H. (1953). *Acta Metall.* pp. 122–131.